Structural, Electronic and Magnetic Properties of Silicene Substituted with Monomers and Dimers of Cr, Fe and Co

M. DavoodianIdalik, A. Kordbacheh*
Materials Simulation Laboratory, Department of Physics,
Iran University of Science and Technology, Tehran, Iran

ABSTRACT

Extensive full-potential density functional theory calculations were performed to investigate the structural, electronic and magnetic properties of silicene substituted with monomers and dimers of Cr, Fe and Co atoms. Different concentrations of monomers between 1 and 12 percent were considered. The structures substituted with all concentrations of Fe were metal and showed magnetic properties. The structures substituted with Co and Cr were half-metal or metal and, surprisingly, silicene substituted with 1.4 percent Co did not show a magnetic moment. Homonuclear and heteronuclear dimers of the above atoms were investigated for two different substitution positions in silicene. The structures showed metallic or half-metallic properties and a range of magnetic moments from 0 to 6 μ_B. This variety of electronic and magnetic properties suggest that metal-substituted silicene materials could play essential roles in nano-electronic devices in fields such as spintronics.

1. INTRODUCTION

More than a decade has passed since the discovery of graphene [40]. During this period of time, the advantageous and unique properties of graphene have been investigated, and atomically two-dimensional (2D) materials have arisen as a subject of research in nanoscale materials science. Silicene, on the other hand, is the graphene equivalent of silicon with a buckled crystal structure due to sp3 hybridization. Silicene has attracted considerable attention from scientists and engineers as an alternative to graphene, primarily because of the compatibility of silicene with current silicon-based electronic devices. The first hints of the possibility of fabricating silicene (as nanoribbons) on silver substrates were provided after a few fairly obscure theoretical studies on silicene and its general properties [2,11,15,28,52]. Some of the remarkable properties of silicene revealed by theoretical and experimental investigations include: large spin–orbit coupling at the Dirac point of 1.5 meV [8,33,34], in contrast to that of graphene (24 μeV) [1,17]; quantum spin and quantum anomalous Hall effects [12,33,45]; electrically tunable band gap [7,10,39,58]; transition from a topological insulating phase to a band insulator under electric field or strain [13,31,56]; and tunable band gap under strain [9,10,21,38,39,43,44].

The 2D nature of silicene makes it possible to tune its characteristics to introduce impurities such as adsorbing or substituting atoms. In numerous investigations, defects have been patterned into silicene to modify the electronic and magnetic properties of the structure

*Corresponding Author: akordbacheh@iust.ac.ir

or enhance the diversity of attainable properties. The functionalization of silicene has been shown to significantly influence the band structure and magnetic properties of the system [6,14,16,20,30,53,54,59]. For instance, when non-magnetic silicene is half-hydrogenated, it changes into a ferromagnetic semiconductor [59]. Moreover, the metal atoms interact strongly with silicene because of its buckled hexagonal structure. This interaction depends on the type and atomic radius of the adatom; thus, silicene can exhibit the behavior of a metal, half-metal or semiconductor [32,47]. Lin et al. found that when the silicene surface is functionalized with adatoms like Li, Na, k, Ca, Co, Ni, Pd and Pt, a large binding energy is obtained compared to the cohesive energy of the bulk metal. Au and Sn bind strongly and covalently to silicene, whereas their binding with graphene is weak. This binding energy is appropriately ionic for the adatoms of alkali metals on silicene [18,47]. The substitution of Si by B, N, Al or P atoms in silicene nanoribbons has been shown to result in ferromagnetic character of the system, which can be attributed to the perturbation of p and p* states localized at the doped edges [23,35,36,60,61]. Furthermore, the adsorption of homonuclear and heteronuclear dimers has been shown to result in exotic physical properties. B. Mohan et al. showed that while the adsorption of homo-dimers of B, C and N results in semiconductor behavior, the hetero-dimers of B-C and C-N produce metallic behavior, in contrast to the absorption of B and N monomers, which does not result in band gap opening [37]. In a theoretical study, H. Johll et al. carried out density functional theory (DFT) calculations to study the adsorption site configuration and stabilities, magnetic moments and band structures of ferromagnetic elements Fe, Co and Ni as adatoms and homonuclear dimers adsorbed on silicene; they found that the adsorption energies of the above elements were greater compared to on graphene [22]. In addition, they observed a small band gap induction from the adsorption of the metal adatoms on silicene, with Co adatom having the largest spin-polarized band gap.

As traditional 3d magnetic elements, Cr, Fe, Co and Ni have attracted considerable interest in recent years because of their enhanced magnetization diversities, high spin polarization, strong binding as adatoms with 2D materials, and so on, making them a potential material candidate for use in data storage and spintronic applications. These metals are economical and, because of their degree of spin polarization, can supply spin-polarized carriers. Although few theoretical studies have been carried out on the electronic and magnetic properties of single silicene layers with adsorbed monomers and dimers of these atoms, the variety of their applications necessitates more investigations. In this paper, we present a DFT study of traditional metal atoms, Cr, Fe and Co, embedded as monomers and dimers in monolayer silicene. To provide a comprehensive comparison, all possible configurations of the atoms have been investigated, and different concentrations between 1 to 12 percent have been considered for the monomer substitution of these three atoms in silicene. The substitution of dimers has been investigated in two different positions: interlayer and intralayer. The paper is organized as follows. The computational methods are described in Section 2. The electronic and magnetic properties of monomer-substituted structures are presented in Section 3. In Section 4, the dimer-substituted structures are investigated. The results are summarized in Section 5.

2. COMPUTATIONAL METHODOLOGY

We employed spin-polarized DFT with the WIEN2k code, which is based on the full-potential linearized augmented plane wave plus local orbitals approach [3]. Electronic exchange-correlation effects were simulated using the generalized gradient approximation (GGA) of Perdew, Burke and Ernzernhof (PBE)[42]. The potential and charge density of the full potential were expanded by spherical harmonics inside the muffin-tin spheres and by plane-wave basis sets in the interstitial region. The Brillouin zone sampling was performed using an 18 × 18 × 1 Monkhorst-Pack grid for self-consistent calculations. All atomic positions were optimized by minimizing the total energy and atomic forces to 10-7 Ry and 1.0 mRy/au, respectively. The plane-wave cut-off value and Fourier expansion value were chosen to be 12 Ry and 144 Ry, respectively.

To obtain structures with different concentrations of one impurity atom, we substituted Cr, Fe and Co atoms in supercells with 8 (2 × 2), 18 (3 × 3), 32 (4 × 4), 50 (5 × 5) and 72 (6 × 6) atoms. For monomer substitution, one Si atom in the supercell was replaced by one impurity atom. For the substitution of dimer compounds, a 4 × 4 supercell (30 Si atoms and two impurity atoms) was chosen. The monomers and dimers of impurity atoms were displaced slightly away from the high-symmetry sites to avoid the local minima.

To avoid interaction between silicene layers, a vacuum layer of 29 Bohr was added normal to the silicene plane in the Z direction.

3. MONOMER SUBSTITUTION

Pure silicene has been reported to have a buckling height of 0.43 to 0.54 Å, and the Si–Si bond length is between 2.25 and 2.29 Å [4,19,26,32,34,41,46]. The freestanding silicene in these calculations had a buckling height of 0.48 Å and an Si–Si bond length of 2.26 Å.

First, different concentrations of impurity atoms were considered. One impurity atom was substituted for one Si atom, and the structure was relaxed. Because of the special geometry of silicene, local minimization may occur. Thus, the impurity atom was added from both sides of the silicene plane (at the top and bottom of the removed Si atom), and the relaxed structure with minimum energy was chosen.

The typical atomic configuration of silicene substituted with one impurity atom is shown in Figure 1. Since the covalent radii of transition metal (TM) atoms like Cr, Fe and Co are larger than that of Si, the substituted atoms are displaced from the silicene layer. This behavior has also been observed in TM-substituted graphene [25,27,50,55].

The formation energies were calculated as below:

$$E_f = E_{total} - N_i \times E_i - N_{Si} \times E_{Si}$$

where E_f is the formation energy, E_{total} is the total energy of the relaxed structure, N_i is the number of impurity atoms in the supercell, E_i is the energy of the impurity atom(s), N_{Si} is the number of silicon atoms in the supercell, and E_{Si} is the energy of one silicon atom. The stabilities of these structures are an important topic for fabrication and application in silicon-based electronics; in this paper, the properties of the stable structures are investigated.

The TM–Si lengths, buckling height, formation energies and total magnetic moments (TMMs) of silicene structures substituted with different concentrations of Cr, Fe and Co are shown in Table 1.

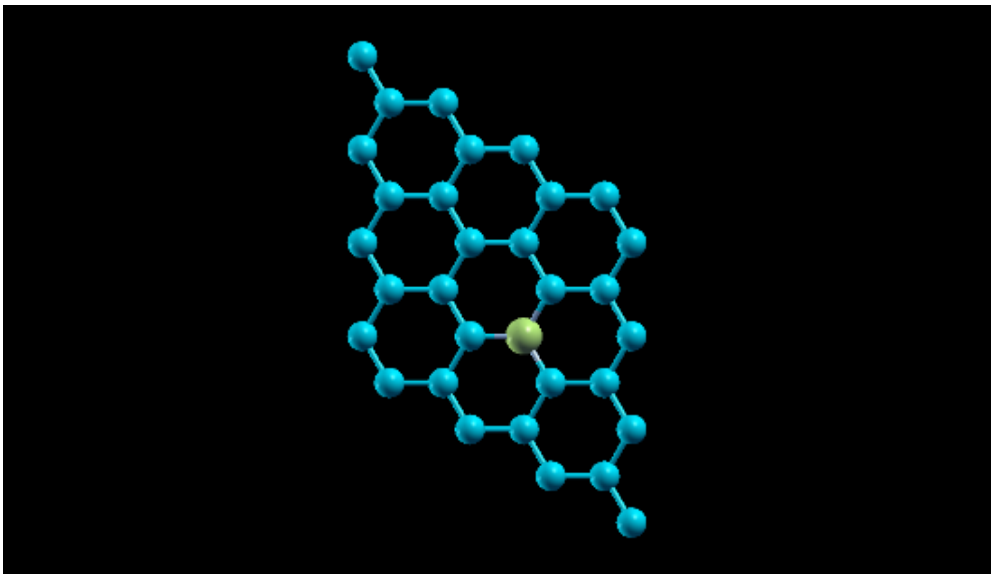

Figure 1 Substitution of an impurity atom in a silicene plate

Table 1 Properties of silicene structures substituted with different concentrations of Cr, Fe and Co

Structure (impurity percent %)	**Impurity atom**	**Formation Energy (Ry/atom)**	**TM–Si length (Å)**	**Buckling Height (Å)**	**Total Magnetic Moment (μ_B)**
2 in2 (12.5)	Cr	-0.2995	2.26	1.12	2
	Fe	-0.2812	2.21	1.21	2.2
	Co	-0.2773	2.19	1.16	1
3 in 3 (5.5)	Cr	-0.2891	2.26	1.52	2
	Fe	-0.2801	2.19	1.26	0.3
	Co	-0.2806	2.19	1.13	1.3
4 in 4 (3.1)	Cr	-0.2741	2.25	1.88	2
	Fe	-0.2503	2.2	1.43	0.5
	Co	-0.2787	2.19	1.17	1
5 in 5 (2)	Cr	-0.2445	2.26	1.98	2
	Fe	-0.2555	2.18	1.72	0.6
	Co	-0.2617	2.17	1.15	0.4
6 in 6 (1.4)	Cr	-0.2107	2.26	1.777	2.1
	Fe	-0.1533	2.20	1.64	0.8
	Co	-0.1103	2.21	1.63	0

A glimpse at the table reveals that the buckling height for Co does not change significantly with Co concentration, while for Fe and Cr, it increases with the structure dimensions. Among these three transition metals, the structures substituted with Cr are more buckled. The bond lengths between these impurity atoms and the nearest-neighbor Si atoms do not change dramatically with concentration, and Cr has the biggest Si–M distance. The TM–Si bond length and elevated height of the impurity monomers in the silicene layer generally reflect the

size of the TM atom. In the structures with Cr as the impurity atom, only the substituted Cr atom was removed from the structure. In contrast, for the other impurity atoms, nearby Si atoms came out along with the substituted atom. Compared with Co-substituted graphene [48], the Co–Si bond length in silicene is approximately 0.4 Å more than that in graphene, likely because of the larger atomic radius of silicon atom. In general, the Si–M bond lengths in silicene with substituted metal atoms are smaller than those in metal-adsorbed silicene (Table 2).

Table 2 Average TM distance to the nearest Si(C) atoms in adsorbed and substituted silicene and graphene from different references and this work

	Metal-Added graphene [23] ([5])	**Metal-Added Silicene[22,24]**	**Metal-Substituted Graphene[27]**	**Metal-Substituted Silicene**
Cr	-	2.3	2.02	2.25
Fe	1.54 (2.11)	2.3	1.96	2.2
Co	1.51(2.10)	2.3	1.94	2.19

Investigation of the formation energies for the substitution of different concentrations of monomers shows that the Cr-substituted structures have the highest formation energies among the three TMs, and formation energy decreases from Cr to Co. The hybridization with the silicone vacancy states near the Fermi energy level is reduced as the 3d shell becomes occupied and moves towards lower energy, thereby decreasing the binding energy. For different impurity concentrations, the formation energy increases as concentration increases (for clarification, the formation energies are shown in Figure 2). The formation energies found in this study are larger than those for smaller atoms like B, N or P [51]. These considerable formation energies indicate strong interactions between the TM atoms and their nearest-neighbor Si atoms.

The up and down band structures of the silicone substituted with different concentrations of Cr are shown in Figure 3 as an example. The general schematic of the band structure for all impurity atoms is the same; with decreasing impurity concentration, the effect of the TM atoms on the properties of the structure is reduced, and the structures show more similar schemes. This is not true for graphene, which is less dependent on the size of the supercell [49]. The crossing band of pure silicene at the K symmetry point is removed for these monomers because of the strong interaction with the d states of the metal atoms.

For all Fe concentrations, the Fe-substituted structures are metal and high concentration (5.5 and 12.5 percent) of Cr-substituted structures are half-metal. Although GGA DFT is known to underestimate band gaps, some of the above half-metal structures may be categorized as non-metal in nature. The interesting point of these band structures is that in the low concentration (1.4 and 2 percent) of Fe and Co, there is a transport middle band at the Fermi level, which can be used as special electronic and spintronic devices.

For the adsorption of Cr, Fe and Co atoms to silicene, the preferred position is hollow site on top of silicone hexagons, and the structures with Cr, Fe and Co atoms are half-metal, semiconductor and metal, respectively [47]. In another study [22], the Fe- and Co-adsorbed structures were found to be non-metal with small band gaps of approximately 0.04 and 0.7 eV (0.06 and 0.28 eV for minority spins) at the k-point, respectively. However, when these atoms are substituted into a 4 in 4 silicene structure, they show metallic properties.

We also present the total and partial density of state (PDOS; major and minor) for all concentrations of Co impurities. The PDOS analysis of all concentrations of Co impurities

revealed strong hybridization between the substituted atom and the nearby Si atoms of the sheet, resulting in the deformation of the Dirac cone of pristine silicene. These metal atoms drastically modify the silicene electronic structure, and the states around the Fermi level mainly arise from the d orbitals of substituted 3d atoms. In graphene, when cobalt or iron atoms are added to graphene as adsorption atoms, the DOS opens a gap of approximately 0.2 eV for the majority spin but remains continuous for the minority spin [5]. For Cr- and Fe-embedded graphene, the structures have small band gaps; for Co-embedded graphene, the structure band is spin polarized and have a little gap for minority spins[49]. As stated earlier, for the adsorption of Cr, Fe and Co on silicene, the structures are half-metal, semiconductor and metal, respectively [47].

The investigation of the TMMs of the silicene structures indicated that the TMMs of the structures with Cr impurity atoms were approximately 2 μ_B for all concentrations. The Cr-substituted structures had the largest Si–M distances for all tested concentrations. The effect of Cr absorption did not change significantly with Cr concentration. In fact, for Cr, the non-bonding 3d levels become populated, giving rise to strong localized d character and a 2-μ_B spin moment. At concentrations of 3 to 12 percent, Co Impurities induced TMMs of approximately 1 μ_B; the TMM decreased to almost zero at the Co concentration of 1 percent, and the characteristic silicene states were maintained at the low impurity concentrations. This behavior is similar the report of lan et al., who found that TMM changed between 0 and 1 μ_B for different positions [29]. The TMMs of structures containing Fe impurity atoms were less than 1 μ_B, in agreement with the work of Zheng et al. [62,63].

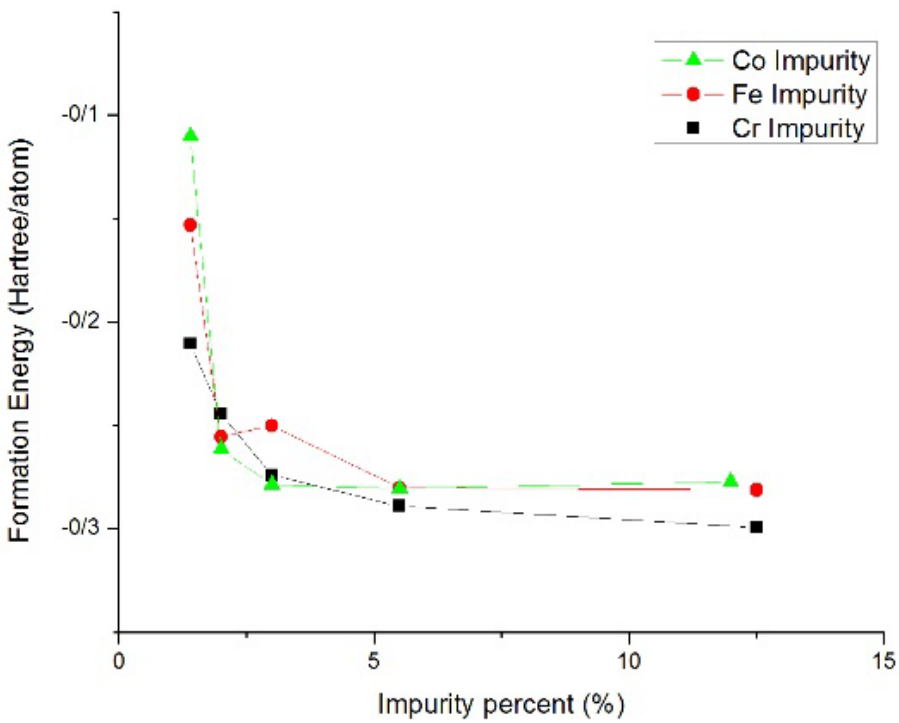

Figure 2 Formation energies of silicene substituted with different concentrations of Cr, Fe and Co

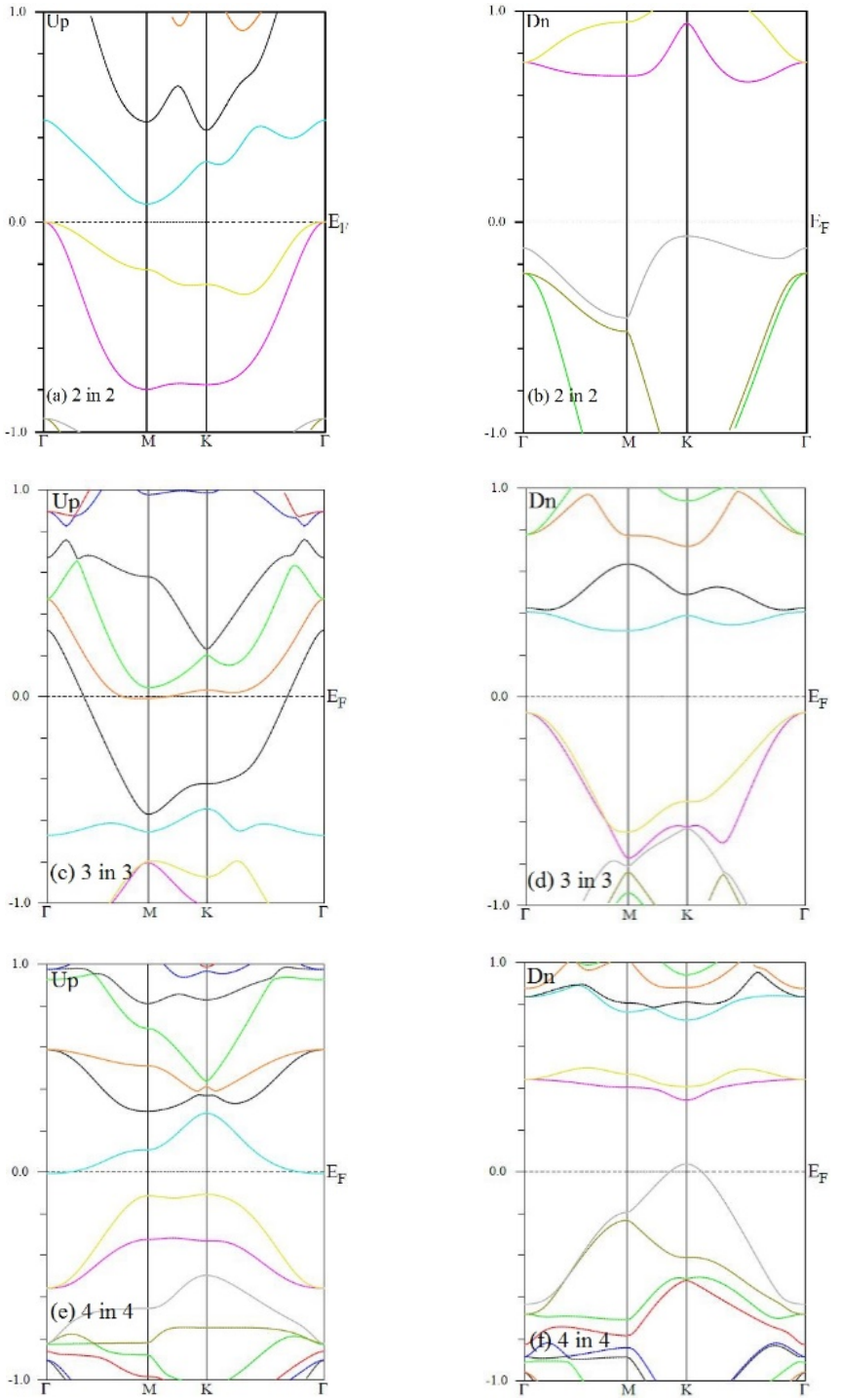
Up
Dn
(a) 2 in 2
(b) 2 in 2
(c) 3 in 3
(d) 3 in 3
(e) 4 in 4
(f) 4 in 4
1.0
0.0
-1.0
Γ
M
K
E_F

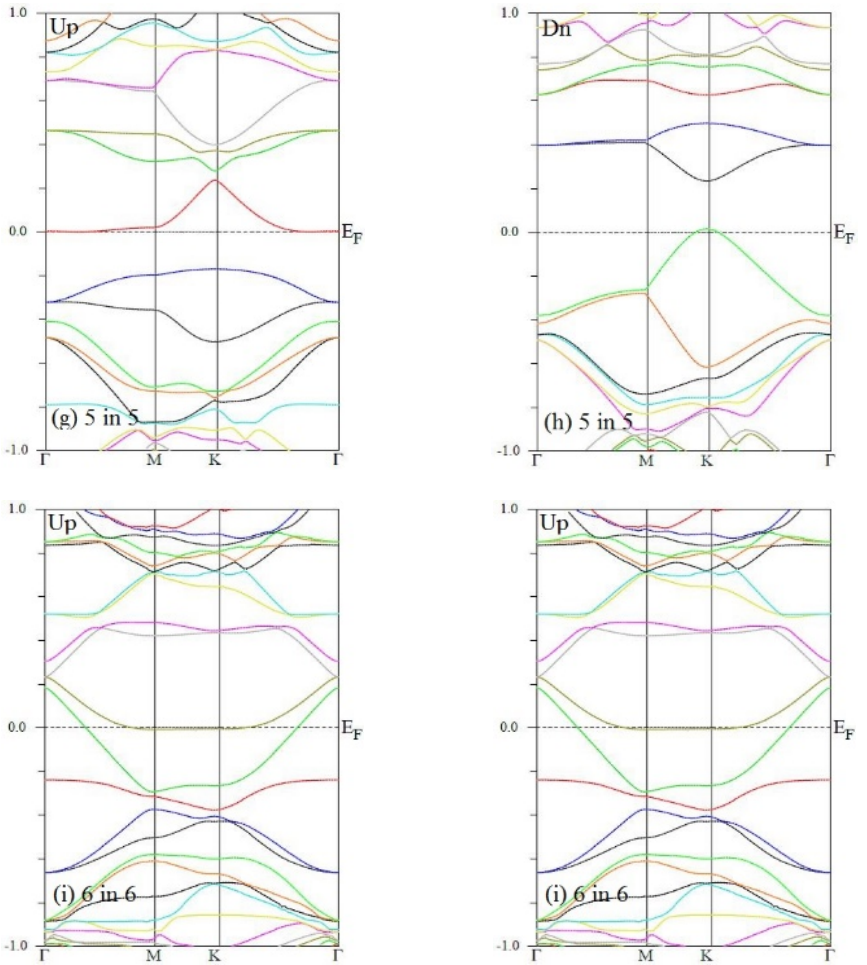

Figure 3 Band structures for silicene substituted with different concentrations of Cr

4. DIMER SUBSTITUTION

Dimer substitution results in more complex structures compared to monomer substitution. Dimers can be homonuclear or heteronuclear (as described in the next parts), and the substitution positions of these dimers in silicene can be different. For dimers of impurity atoms, the following two different dimer positions in a 4 in 4 supercell have been considered:

1) In-plane (intralayer) substitution where two impurity atoms substitute for two silicone atoms, and each atom of the dimer binds to the two nearest Si atoms of the silicene plate (Figure 4). Table 3 presents the formation energies, average TM–Si bond length, buckling height and metal type of the intralayer dimer-substituted silicene structures.
2) Normal (interlayer) substitution where two impurity atoms substitute for one Si atom perpendicular to the silicene plane. In this structure, each atom of the dimer can bind to the three nearest Si atoms (Figure 5). In addition, because of the buckling height of

silicene, there are two different permutations of the two atoms of one heteronuclear dimer. This means that the exchange of the two impurity atoms of a dimer are not equivalent; accordingly, in perpendicular form, there are a total of six different structures for heteronuclear dimers and three different structures for homonuclear dimers. The properties of interlayer dimer-substituted silicene structures are presented in Table 4.

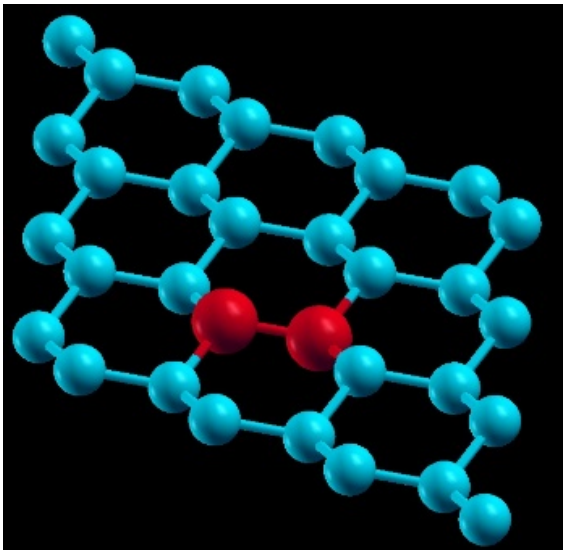

Figure 4 Intralayer substitution of a dimer in silicene

Table 3 Formation energies, average TM–Si bond length, buckling height and the metal type of intralayer dimer-substituted silicene (M: metal; H: half-metal)

Homo/Hetero-Nuclear	**Dimer**	**Formation Energy (Ry/atom)**	**TM–Si Length (Å)**	**Buckling Height (Å)**	**Magnetic Moment (μ_B)**	**Metallicity**
Homonuclear	Cr-Cr	-0.2548	2.27	1.22	0	M
	Fe-Fe	-0.2365	2.21	1.23	5	M
	Co-Co	-0.2186	2.12	0.18	2.9	M
Heteronuclear	Fe-Cr	-0.2419	2.23	1.23	2	M
	Co-Cr	-0.2411	2.26	1.65	3	H
	Fe-Co	-0.2390	2.8	1.81	3.3	M

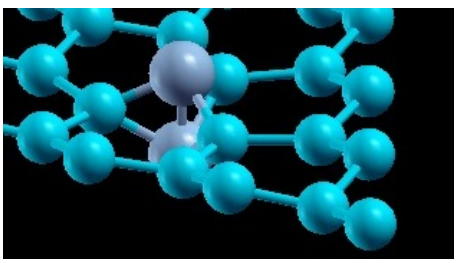

Figure 5 interlayer substitution of a dimer in silicene

Table 4 General properties of interlayer dimer-substituted silicene (Cr, Fe and Co). Dimer notation is A-B sign, where A represents the down impurity atom, and B is the up impurity atom (M: metal; H: half-metal)

Homo/Hetero-Nuclear	Dimer	Formation Energy (Ry/atom)	Average TM–Si Length (Å)	Buckling Height (Å)	Magnetic Moment (μ_B)	Metallicity
Homo	Cr-Cr	-0.2673	2.35	1.97	2	H
	Fe-Fe	-0.2744	2.23	2.07	6	H
	Co-Co	-0.2751	2.24	2.40	1	M
Hetero	Cr-Fe	-0.2595	2.29	1.94	4	H
	Fe-Cr	-0.2646	2.29	1.97	4	H
	Cr-Co	-0.2725	2.28	2.07	3	H
	Co-Cr	-0.2601	2.29	2.08	4.2	M
	Fe-Co	-0.2514	2.23	2.17	3.7	M
	Co-Fe	-0.2755	2.24	2.37	3.1	M

4.1. Homonuclear dimers

The average Si–M bond lengths of the silicene structures substituted with one impurity atom are 2.25, 2.2 and 2.12 Å for Cr, Fe and Co, respectively. When two similar impurity atoms are substituted for two silicon atoms to form an intralayer homonuclear dimer, the average Si–M bond length become 2.27, 2.2 and 2.12 Å for Cr, Fe and Co, respectively. This is because of the dimer bonding length, which increases from Cr to Co, pushing impurity atoms nearer to silicon atoms. In the interlayer homonuclear dimers, the average Si–M bond lengths for the up and down atoms of the dimers are similar (difference less than 0.05 Å); the bond lengths are approximately 2.35, 2.23 and 2.35 Å for Cr, Fe and Co dimers, respectively.

Here, the structures with Fe as the impurity atom are presented as an example. The free Fe dimer bond length has been reported as 1.96 Å [22]. For Fe dimer adsorbed on silicene, the most stable configuration is the b-atom site-hole site configuration. The bond length of the Fe dimer and the distance from Fe to the nearest Si atom are both 2.3 Å [22]. In our calculations, the bond lengths for the free, intralayer and interlayer Fe dimers are 2.01, 1.97 and 2.07 Å, respectively. The Fe-dimer bond length of the interlayer substituted silicene is the same as the dimer added to graphene layer in which, the preferred position is perpendicular (PBE calculations) [5]. In silicene substituted with intralayer Fe dimer, the symmetry of the system causes the two Fe atoms to be equivalent, and the PDOS of the Fe atoms are identical.

The silicene structure substituted with interlayer Fe dimer (Cr dimer) is a half-metal since the band structure shows an indirect energy gap of 0.4 (0.31) eV for the minority (majority) spin channel in our calculation and no energy gap for the majority (minority) spin channel (Figure 6).

It has been reported that the most stable configurations for Fe dimer adsorption open a spin-polarized band gap [22]. Here, for the intralayer configurations of Fe-dimer (Cr-dimer) substitution, there is no spin-polarized band gap. The above discussion is true for Co homonuclear structures; however, they are metal for both intralayer and interlayer silicenes.

The investigation of the formation energies for Cr, Fe and Co homonuclear dimers in intralayer and interlayer structures shows the following. First, silicene with intralayer Cr dimer has the highest formation energy among structures with intralayer dimers. The formation

energy decreases from Cr to Co with decreasing Si–M distance and increasing dimer bond length. Second, for perpendicular homonuclear substituted dimers, the formation energy (per atom) increases from Cr to Co with increasing dimer bond length. Third, the difference in formation energy between the dimers in intralayer and interlayer silicene structures shows that the structures with perpendicular homonuclear dimers have greater formation energies compared to the same dimers in intralayer structures, for which there are two Si–TM bonds for each TM atom.

The magnetic moment of a free Fe dimer is 6 μ_B . In silicene with adsorbed Fe dimer, TMM is about 6 μ_B [22,47]. Here, the TMM of the intralayer Fe dimer-substituted structure is about 5 μ_B, while that of the interlayer structure is about 6 μ_B. This difference results from the charge difference between the structures. For vertical substitution, each Fe atom possesses less than seven electrons on its five 3d orbitals after orbital hybridization; thus, electrons remain unpaired are not three, and the local magnetism of the Fe atoms are about 2.2 and 2.3 μ_B for down and up atoms, respectively. Although this is true for the parallel Fe dimer substitution, the TMM decreases to approximately 5 μ_B. We should mention that there is a configuration for vertically stacked at hole site of the silicene with about 0.68 eV less adsorption energy than the most stable structure which has 6 μ_B [22]. Therefore, it can be compared to the structure substitutes with vertical Fe dimer.

Although the TMM of the perpendicular homonuclear Cr dimer-substituted structure is about 2 μ_B, it decreases to about zero when the Cr dimer is parallel to the silicene plate. The TMM of the silicene with perpendicular substituted Co dimer is about 3 μ_B, which again decreases to about 2 μ_B when the dimer is parallel to silicene.

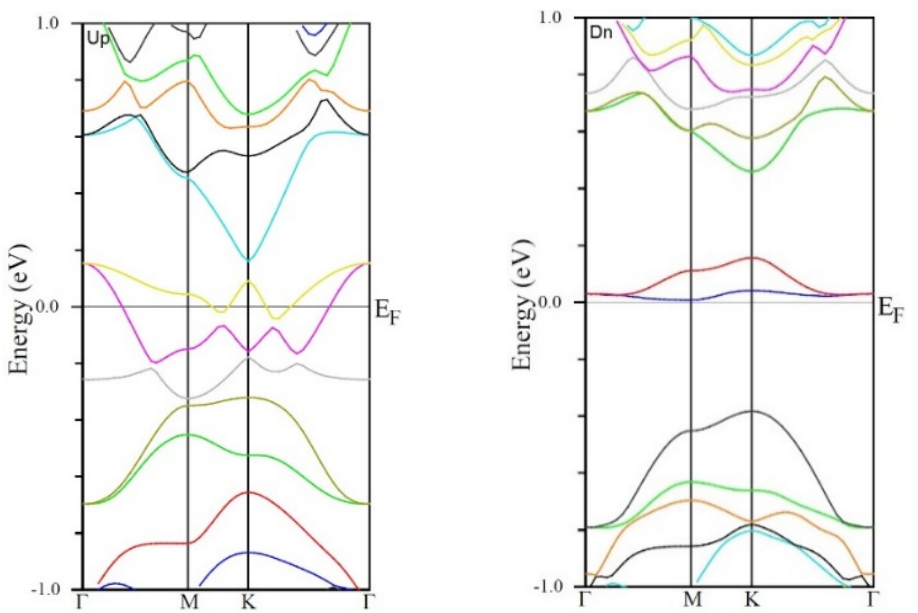

Figure 6 The majority and minority band structures of silicene doped with interlayer Fe dimer

4.2. Heteronuclear dimers

Tables 3 and 4 show that the interlayer structures with heteronuclear Co-Fe dimers (Co down and Fe up) and Fe-Co (Fe down and Co up) have the largest dimer bond lengths regardless of which atom is up or down. The dimer bond length is the smallest for Cr-Fe dimer (Cr down and Fe up), and the Fe-Cr dimer (Fe down and Cr up) has the second smallest bond length. In general, Cr–Si bonds are the longest. Co has the shortest Si–metal bond length among these three atoms because the atomic radius decreases from Cr to Co. As in these structures, the dimers are perpendicular to the silicene plate, and the atoms of the dimers are more elevated than the Si atoms. The buckling heights of the structures are equal to the dimer lengths. Therefore, the structure with Co-Fe dimer has the largest buckling height. This is not consistent with the structures substituted with only one impurity atom, for which neither the Fe- nor Co-substituted structures have the greatest buckling height.

The formation energies per atom of the interlayer dimer-substituted structures show that all the structures are stable. In general, the formation energies of homonuclear structures are greater than those of the heteronuclear ones. Among the interlayer heteronuclear structures, the structure substituted with Co-Fe dimer has the maximum formation energy. The homonuclear perpendicular Co dimer-substituted structure has the greatest formation energy, and the Co atom binds strongly to three nearby silicon atoms. Here, the interlayer heteronuclear structures with Co atoms have high binding energies and are stable, likely because of the low interconfigurational energy of Co atom. For Co, the experimental interconfigurational energy for the transfer of one electron from an s orbital to a d orbital (i.e. $3d^{n-2}4s^2 \rightarrow 3d^{n-1}4s^1$) is -0.03 eV [57]. This is not true for intralayer structures which less atomic radius of Co and the Si–M bond length change the Si–Si bond length of pristine silicene drastically and the structures with intralayer substituted Co dimer have less formation energies.

The band structures and PDOS analyzing of heteronuclear structures in intralayer and interlayer forms show that four structures of nine different structures are half-metal, five structures of them have no band gap and are metal. Figure 7 shows the band structure and density of state for interlayer Cr-Co dimer as an example. The interlayer and intralayer structures substituted with heteronuclear dimers of Cr-M and M-Cr, except intralayer Co-Cr, are half-metals. The Cr atom is the common atom in these structures, and the half-metal property comes from this atom. In the structures substituted with one impurity, a few of the Cr-substituted structures also exhibited half-metal properties.

The TMMs of the interlayer and intralayer heteronuclear dimer-substituted structures are shown in Tables 3 and 4. The magnetic moments are related to features in the electronic band structure; thus, they should respond to changes in the Fermi level. The TMMs for the interlayer Cr-Fe and Fe-Cr dimers are about 4 μ_B. As the M–Si bonds do not change drastically upon changing the atoms of the dimer in the structure, the TMMs of the Cr-Fe and Fe-Cr interlayer substituted structures are similar. This is also true for Fe-Co (Cr-Co) and Co-Fe (Co-Cr). In intralayer structures, every atom of the dimer bonds with two nearby Si instead of three, as in the interlayer structures. The TMM for the dimer with Co as the down atom and Cr as the up atom is about 4.2 μ_B, which decreases to 3 μ_B upon changing the positions of the dimer atoms. The TMM for Fe-Co dimer is 3.7 μ_B, which again decreases to 3.1 μ_B for Co-Fe. The difference in the TMMs of the interlayer and intralayer structures is attributed to the different

electronic interactions and charge transformations between the impurity atoms in different positions and the pristine silicene layer.

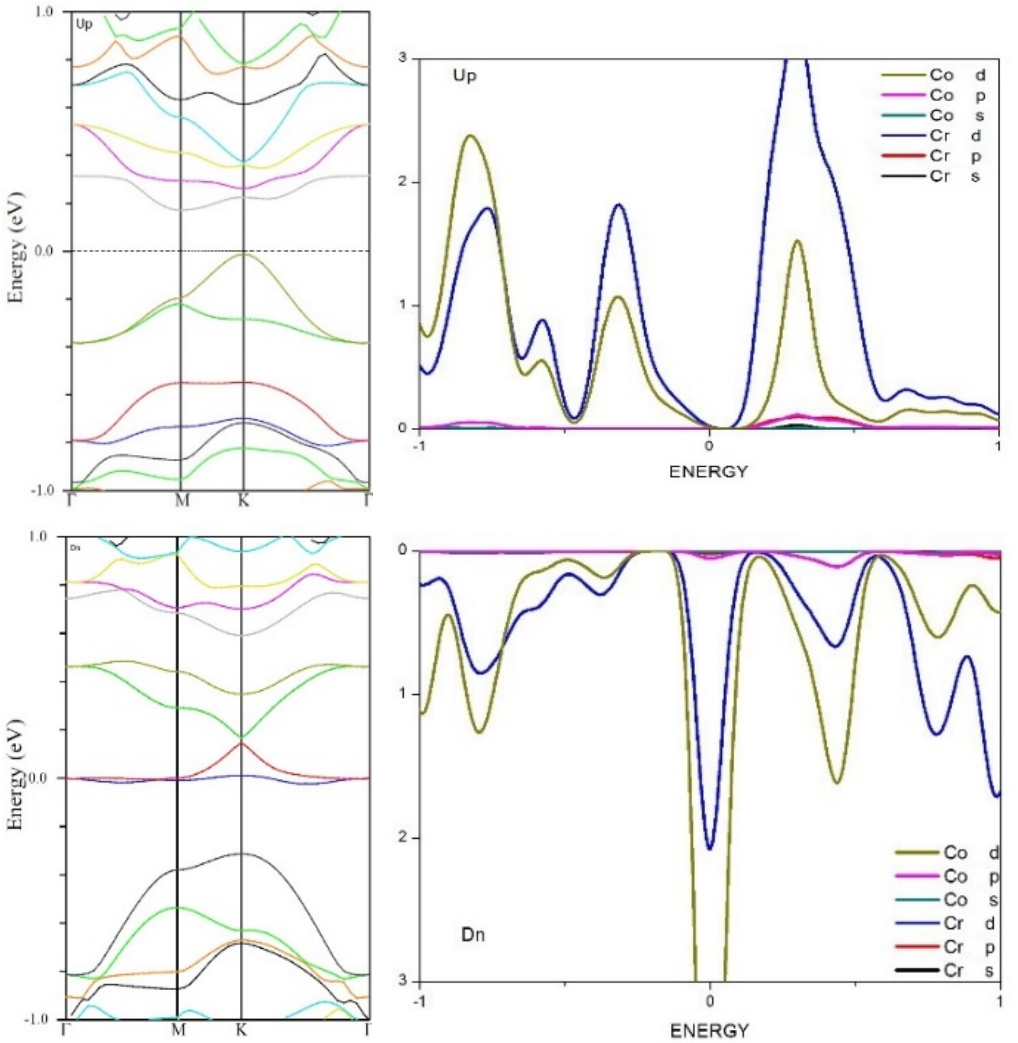

Figure 7 Majority and minority band structures and PDOS of silicene substituted with interlayer Cr-Co dimer

5. CONCLUSION

In summary, using spin-polarized DFT, we examined the structural, electronic and magnetic properties of 2D, low-bucked silicene substituted with monomers and dimers of Cr, Fe and Co atoms.

The substitution of monomers was performed for monomer concentrations from 1 to 12 percent. The numerical studies revealed that high concentrations of Co and Cr atoms produce half-metal structures, while low concentrations result in metal structures. The formation energies are the greatest for the structures with Cr atom as the impurity and decrease from Cr

to Co. For different impurity concentrations, the formation energy decreases from as concentration decreases. The silicene structures substituted with all concentrations of Fe are metal. The TMMs of the structures show that the structures substituted with high concentrations of Co are 1 μ_B, which decreases to zero for low concentrations of Co. The TMMs of Fe-substituted structures are between 0.3 and 2 μ_B. The Cr-substituted structures have TMMs of 2 μ_B for all Cr concentrations.

Dimers were categorized in two classes, homonuclear and heteronuclear, which assume two different substitution positions: in the plane (intralayer) and normal to the plane (interlayer) of silicene. All the intralayer homonuclear dimers have no band gap in their band structures and are metal. Unlike the monomer Cr-substituted structures, the intralayer Cr dimer-substituted structures have no magnetic moment. The structure containing Fe dimer has a TMM of about 5 μ_B, and the TMM of the structure substituted with Co dimer is about 3 μ_B.

The structure substituted with the interlayer homonuclear dimer of Cr is half-metal, and its TMM is about 2 μ_B, which is different than that of the intralayer structure. The TMM of the interlayer Fe dimer-substituted structure is about 6 μ_B, which decreases to 5 μ_B for the intralayer structure. The interlayer structures with Co dimers have no band gaps and are metal. Interestingly, the interlayer structure of the Co dimer has a TMM of about 2 μ_B, lower than that of the intralayer structure.

There are six different interlayer heteronuclear dimers of these three atoms, and three of them are half-metal. The Cr atom is the common atom in these three half-metal structures. The obtained TMMs for these six structures range from 3.1 to 4.2 μ_B. The heteronuclear structures with Fe and Co atoms have the greatest TMMs among these structures. The intralayer heteronuclear structures with Fe-Cr, Co-Cr and Fe-Co dimers are metal, half-metal and metal, respectively, and their TMMs vary from 2 to 3.3 μ_B. The variety of electronic and magnetic properties observed in this study suggest that monomer- and dimer-substituted silicene may have applications in nano-electronic devices in fields like spintronics.

REFERENCES

[1] Samir Abdelouahed, A. Ernst, J. Henk, I. V. Maznichenko, and I. Mertig. 2010. Spin-split electronic states in graphene: Effects due to lattice deformation, Rashba effect, and adatoms by first principles. Phys. Rev. B 82, 12 (September 2010), 125424.

[2] Bernard Aufray, Abdelkader Kara, Sébastien Vizzini, Hamid Oughaddou, Christel Léandri, Benedicte Ealet, and Guy Le Lay. 2010. Graphene-like silicon nanoribbons on Ag(110): A possible formation of silicene. Appl. Phys. Lett. 96, 18 (May 2010), 183102.

[3] P Blaha, K Schwarz, and GKH Madsen. 2001. WIEN2K, An Augmented Plane Wave+ Local Orbitals Program for Calculating Crystal Properties (TU Wien, Austria, 2001). ISBN 3-9501031-1-2 (2001), 2001.

[4] S Cahangirov, M Topsakal, E. Aktürk, H. Şahin, and S Ciraci. 2009. Two- and One-Dimensional Honeycomb Structures of Silicon and Germanium. Phys. Rev. Lett. 102, 23 (June 2009), 236804. DOI:https://doi.org/10.1103/PhysRevLett.102.236804

[5] Chao Cao, Min Wu, Jianzhong Jiang, and Hai-Ping Cheng. 2010. Transition metal adatom and dimer adsorbed on graphene: Induced magnetization and electronic structures. Phys. Rev. B 81, 20 (2010), 205424.

[6] Guohua Cao, Yun Zhang, and Juexian Cao. 2015. Strain and chemical function decoration induced quantum spin Hall effect in 2D silicene and Sn film. Phys. Lett. Sect. A Gen. At. Solid State Phys. 379, 22–23 (2015), 1475–1479.

[7] Son-Hsien Chen. 2016. Electrically tunable spin polarization in silicene: A multi-terminal spin density matrix approach. J. Magn. Magn. Mater. 405, (May 2016), 317–323.

[8] Suman Chowdhury and Debnarayan Jana. 2016. A theoretical review on electronic, magnetic and optical properties of silicene. Reports Prog. Phys. 79, 12 (December 2016), 126501.

[9] Ning Ding, Huan Wang, Xiangfeng Chen, and Chi-Man Lawrence Wu. 2017. Defect-sensitive performance of silicene sheets under uniaxial tension: mechanical properties, electronic structures and failure behavior. RSC Adv. 7, 17 (2017), 10306–10315.

[10] N. D. Drummond, V. Zólyomi, and V. I. Fal'ko. 2012. Electrically tunable band gap in silicene. Phys. Rev. B 85, 7 (February 2012), 075423.

[11] Hanna Enriquez, Sébastien Vizzini, Abdelkader Kara, Boubekeur Lalmi, and Hamid Oughaddou. 2012. Silicene structures on silver surfaces. J. Phys. Condens. Matter 24, 31 (August 2012), 314211.

[12] Motohiko Ezawa. 2012. Valley-polarized metals and quantum anomalous hall effect in silicene. Phys. Rev. Lett. 109, 05 (2012), 055502.

[13] Motohiko Ezawa. 2012. A topological insulator and helical zero mode in silicene under an inhomogeneous electric field. New J. Phys. 14, 3 (March 2012), 033003.

[14] Rouhollah Farghadan. 2017. Bipolar magnetic semiconductor in silicene nanoribbons. J. Magn. Magn. Mater. 435, (2017), 206–211.

[15] Baojie Feng, Zijing Ding, Sheng Meng, Yugui Yao, Xiaoyue He, Peng Cheng, Lan Chen, and Kehui Wu. 2012. Evidence of silicene in honeycomb structures of silicon on Ag(111). Nano Lett. 12, 7 (July 2012), 3507–11.

[16] Joelson C. Garcia, Denille B. de Lima, Lucy V. C. Assali, and João F. Justo. 2011. Group IV Graphene- and Graphane-Like Nanosheets. J. Phys. Chem. C 115, 27 (July 2011), 13242–13246.

[17] M. Gmitra, S. Konschuh, C. Ertler, C. Ambrosch-Draxl, and J. Fabian. 2009. Band-structure topologies of graphene: Spin-orbit coupling effects from first principles. Phys. Rev. B 80, 23 (December 2009), 235431.

[18] Xi-Xi Guo, Ping Guo, Ji-Ming Zheng, Li-Ke Cao, and Pu-Ju Zhao. 2015. First-principles calculations study of Na adsorbed on silicene. Appl. Surf. Sci. 341, (June 2015), 69–74.

[19] Zhi-Xin Guo, Shinnosuke Furuya, Jun-ichi Iwata, and Atsushi Oshiyama. 2013. Absence and presence of Dirac electrons in silicene on substrates. Phys. Rev. B 87, 23 (June 2013), 235435.

[20] M. Houssa, E. Scalise, K. Sankaran, G. Pourtois, V. V. Afanas'ev, and A. Stesmans. 2011. Electronic properties of hydrogenated silicene and germanene. Appl. Phys. Lett. 98, 22 (May 2011), 223107.

[21] Tian-Tian Jia, Xin-Yu Fan, Meng-Meng Zheng, and Gang Chen. 2016. Silicene nanomeshes: bandgap opening by bond symmetry breaking and uniaxial strain. Sci. Rep. 6, 1 (August 2016), 20971.

[22] Harman Johll, Michael Dao Kang Lee, Sean Peng Nam Ng, Hway Chuan Kang, and Eng Soon Tok. 2014. Influence of Interconfigurational Electronic States on Fe, Co, Ni-Silicene Materials Selection for Spintronics. Sci. Rep. 4, (2014), 7594.

[23] Harman Johll, Jiang Wu, Sheau Wei Ong, Hway Chuan Kang, and Eng Soon Tok. 2011. Graphene-adsorbed Fe, Co, and Ni trimers and tetramers: Structure, stability, and magnetic moment. Phys. Rev. B 83, 20 (May 2011), 205408.

[24] T. P. Kaloni, N. Singh, and U. Schwingenschlögl. 2014. Prediction of a quantum anomalous Hall state in Co-decorated silicene. Phys. Rev. B 89, 3 (January 2014), 035409.

[25] Jun Kang, Hui-Xiong Deng, Shu-Shen Li, and Jingbo Li. 2011. First-principles study of magnetic properties in Mo-doped graphene. J. Phys. Condens. Matter 23, 34 (August 2011), 346001.

[26] Abdelkader Kara, Hanna Enriquez, Ari P. Seitsonen, L.C. Lew Yan Voon, Sébastien Vizzini, Bernard Aufray, and Hamid Oughaddou. 2012. A review on silicene — New candidate for electronics. Surf. Sci. Rep. 67, 1 (January 2012), 1–18.

[27] Krasheninnikov, P. Lehtinen, a. Foster, P. Pyykkö, and R. Nieminen. 2009. Embedding Transition-Metal Atoms in Graphene: Structure, Bonding, and Magnetism. Phys. Rev. Lett. 102, 12 (March 2009), 126807.

[28] Boubekeur Lalmi, Hamid Oughaddou, Hanna Enriquez, Abdelkader Kara, Sébastien Vizzini, Bénidicte Ealet, and Bernard Aufray. 2010. Epitaxial growth of a silicene sheet. Appl. Phys. Lett. 97, 22 (November 2010), 223109.

[29] Mu Lan, Gang Xiang, Chenhui Zhang, and Xi Zhang. 2013. Vacancy dependent structural, electronic, and magnetic properties of zigzag silicene nanoribbons:Co. J. Appl. Phys. 114, 16 (2013), 163711.

[30] L. C. Lew Yan Voon, E. Sandberg, R. S. Aga, and a. a. Farajian. 2010. Hydrogen compounds of group-IV nanosheets. Appl. Phys. Lett. 97, 16 (2010), 163114.

[31] Chao Lian and Jun Ni. 2013. Strain induced phase transitions in silicene bilayers: a first principles and tight-binding study. AIP Adv. 3, 5 (May 2013), 052102.

[32] Xianqing Lin and Jun Ni. 2012. Much stronger binding of metal adatoms to silicene than to graphene: A first-principles study. Phys. Rev. B 86, 7 (August 2012), 075440.

[33] Cheng-Cheng Liu, Wanxiang Feng, and Yugui Yao. 2011. Quantum Spin Hall Effect in Silicene and Two-Dimensional Germanium. Phys. Rev. Lett. 107, 7 (August 2011), 076802.

[34] Cheng-Cheng Liu, Hua Jiang, and Yugui Yao. 2011. Low-energy effective Hamiltonian involving spin-orbit coupling in silicene and two-dimensional germanium and tin. Phys. Rev. B 84, 19 (November 2011), 195430.

[35] Y S Liu, Y J Dong, J Zhang, H L Yu, J F Feng, and X F Yang. 2018. Multi-functional spintronic devices based on boron- or aluminum-doped silicene nanoribbons. Nanotechnology 29, 12 (2018), 125201.

[36] Hang Xing Luan, Chang Wen Zhang, Fu Bao Zheng, and Pei Ji Wang. 2013. First-principles study of the electronic properties of B/N atom doped silicene nanoribbons. J. Phys. Chem. C 117, (2013), 13620–13626.

[37] Brij Mohan, Ashok Kumar, and P. K. Ahluwalia. 2014. Electronic and dielectric properties of silicene functionalized with monomers, dimers and trimers of B, C and N atoms. RSC Adv. 4, 60 (2014), 31700–31705.

[38] Bohayra Mortazavi, Obaidur Rahaman, Meysam Makaremi, Arezoo Dianat, Gianaurelio Cuniberti, and Timon Rabczuk. 2017. First-principles investigation of mechanical properties of silicene, germanene and stanene. Phys. E Low-dimensional Syst. Nanostructures 87, (March 2017), 228–232.

[39] Zeyuan Ni, Qihang Liu, Kechao Tang, Jiaxin Zheng, Jing Zhou, Rui Qin, Zhengxiang Gao, Dapeng Yu, and Jing Lu. 2012. Tunable Bandgap in Silicene and Germanene. Nano Lett. 12, 1 (January 2012), 113–118.

[40] K S Novoselov. 2004. Electric Field Effect in Atomically Thin Carbon Films. Science (80-.). 306, 5696 (October 2004), 666–669.

[41] Tim H. Osborn, Amir a. Farajian, Olga V. Pupysheva, Rachel S. Aga, and L.C. Lew Yan Voon. 2011. Ab initio simulations of silicene hydrogenation. Chem. Phys. Lett. 511, 1–3 (July 2011), 101–105.

[42] John P. Perdew, Kieron Burke, and Matthias Ernzerhof. 1996. Generalized Gradient Approximation Made Simple. Phys. Rev. Lett. 77, 18 (October 1996), 3865–3868.

[43] Rui Qin, Chun-Hai Wang, Wenjun Zhu, and Yalin Zhang. 2012. First-principles calculations of mechanical and electronic properties of silicene under strain. AIP Adv. 2, 2 (2012), 022159.

[44] Ruge Quhe, Ruixiang Fei, Qihang Liu, Jiaxin Zheng, Hong Li, Chengyong Xu, Zeyuan Ni, Yangyang Wang, Dapeng Yu, Zhengxiang Gao, and Jing Lu. 2012. Tunable and sizable band gap in silicene by surface adsorption. Sci. Rep. 2, 853 (November 2012), 1–6.

[45] Majeed Ur Rehman and Zhenhua Qiao. 2018. Assessment of bilayer silicene to probe as quantum spin and valley Hall effect. Eur. Phys. J. B 91, 2 (February 2018), 42.

[46] H. Şahin, S. Cahangirov, M. Topsakal, E. Bekaroglu, E. Akturk, R. Senger, and S. Ciraci. 2009. Monolayer honeycomb structures of group-IV elements and III-V binary compounds: First-principles calculations. Phys. Rev. B 80, 15 (October 2009), 155453.

[47] H. Sahin and F. M. Peeters. 2013. Adsorption of alkali, alkaline-earth, and 3 <math display="inline"> <mi>d</mi> </math> transition metal atoms on silicene. Phys. Rev. B 87, 8 (February 2013), 085423.

[48] E. J.G. Santos, D. Sánchez-Portal, and A Ayuela. 2010. Magnetism of substitutional Co impurities in graphene: Realization of single π vacancies. Phys. Rev. B 81, 12 (March 2010), 125433.

[49] Ejg J G Santos, A Ayuela, and D Sánchez-Portal. 2010. First-principles study of substitutional metal impurities in graphene: structural, electronic and magnetic properties. New J. Phys. 12, 5 (2010), 053012.

[50] Elton J. G. Santos, a. Ayuela, and D. Sánchez-Portal. 2012. Strain-Tunable Spin Moment in Ni-Doped Graphene. J. Phys. Chem. C 116, 1 (January 2012), 1174–1178.

[51] J. Sivek, H. Sahin, B. Partoens, and F. M. Peeters. 2013. Adsorption and absorption of boron, nitrogen, aluminum, and phosphorus on silicene: Stability and electronic and phonon properties. Phys. Rev. B 87, 8 (February 2013), 085444.

[52] Li Tao, Eugenio Cinquanta, Daniele Chiappe, Carlo Grazianetti, Marco Fanciulli, Madan Dubey, Alessandro Molle, and Deji Akinwande. 2015. Silicene field-effect transistors operating at room temperature. Nat. Nanotechnol. 10, 3 (February 2015), 227–231.

[53] Nan Wang, Hao Guo, Yue-jie Liu, Jing-xiang Zhao, Qing-hai Cai, and Xuan-zhang Wang. 2015. Asymmetric functionalization as a promising route to open the band gap of silicene: A theoretical prediction. Phys. E Low-dimensional Syst. Nanostructures 73, (September 2015), 21–26.

[54] Rong Wang, Ming-Sheng Xu, and Xiao-Dong Pi. 2015. Chemical modification of silicene. Chinese Phys. B 24, 8 (2015), 086807.

[55] M Wu, C Cao, and J Z Jiang. 2010. Electronic structure of substitutionally Mn-doped graphene. New J. Phys. 12, 6 (June 2010), 063020.

[56] Yafang Xu, Xingfei Zhou, and Guojun Jin. 2016. Detecting topological phases in silicene by anomalous Nernst effect. Appl. Phys. Lett. 108, 20 (May 2016), 203104.

[57] Susumu Yanagisawa, Takao Tsuneda, and Kimihiko Hirao. 2000. An investigation of density functionals: The first-row transition metal dimer calculations. J. Chem. Phys. 112, 2 (2000), 545.

[58] Xuechao Zhai and Guojun Jin. 2016. Completely independent electrical control of spin and valley in a silicene field effect transistor. J. Phys. Condens. Matter 28, 35 (2016), 355002.

[59] P. Zhang, X.D. Li, C.H. Hu, S.Q. Wu, and Z.Z. Zhu. 2012. First-principles studies of the hydrogenation effects in silicene sheets. Phys. Lett. A 376, 14 (March 2012), 1230–1233.

[60] Xiaojiao Zhang, Dan Zhang, Fang Xie, Xialian Zheng, Haiyan Wang, and Mengqiu Long. 2017. First-principles study on the magnetic and electronic properties of Al or P doped armchair silicene nanoribbons. Phys. Lett. A 381, 25–26 (2017), 2097–2102.

[61] Fu-bao Zheng, Chang-wen Zhang, Shi-shen Yan, and Feng Li. 2013. Novel electronic and magnetic properties in N or B doped silicene nanoribbons. J. Mater. Chem. C 1, 15 (2013), 2735.

[62] Rui Zheng, Ying Chen, and Jun Ni. 2015. Highly tunable magnetism in silicene doped with Cr and Fe atoms under isotropic and uniaxial tensile strain. Appl. Phys. Lett. 107, 26 (2015).

[63] Rui Zheng, Xianqing Lin, and Jun Ni. 2014. The extraordinary magnetoelectric response in silicene doped with Fe and Cr atoms. Appl. Phys. Lett. 105, 9 (2014), 092410.